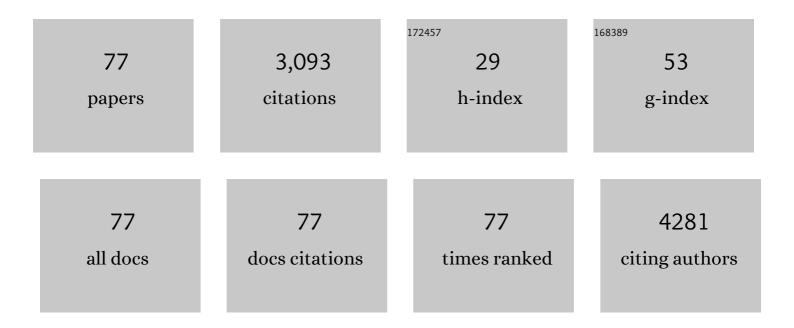
List of Publications by Year in descending order

Source: https://exaly.com/author-pdf/1506477/publications.pdf Version: 2024-02-01



ПСПАМТ

#	Article	IF	CITATIONS
1	Rolling Circle Amplification Combined with Gold Nanoparticle Aggregates for Highly Sensitive Identification of Single-Nucleotide Polymorphisms. Analytical Chemistry, 2010, 82, 2811-2816.	6.5	189
2	Design of Aptamer-Based Sensing Platform Using Triple-Helix Molecular Switch. Analytical Chemistry, 2011, 83, 6586-6592.	6.5	161
3	Upconversion Nanoprobes for the Ratiometric Luminescent Sensing of Nitric Oxide. Journal of the American Chemical Society, 2017, 139, 12354-12357.	13.7	147
4	Exploiting the Higher Specificity of Silver Amalgamation: Selective Detection of Mercury(II) by Forming Ag/Hg Amalgam. Analytical Chemistry, 2013, 85, 8594-8600.	6.5	146
5	Quantitative detection of exosomal microRNA extracted from human blood based on surface-enhanced Raman scattering. Biosensors and Bioelectronics, 2018, 101, 167-173.	10.1	141
6	Design of a Simultaneous Target and Location-Activatable Fluorescent Probe for Visualizing Hydrogen Sulfide in Lysosomes. Analytical Chemistry, 2014, 86, 7508-7515.	6.5	134
7	A colorimetric method for point mutation detection using high-fidelity DNA ligase. Nucleic Acids Research, 2005, 33, e168-e168.	14.5	115
8	Two-Photon Graphene Oxide/Aptamer Nanosensing Conjugate for <i>In Vitro</i> or <i>In Vivo</i> Molecular Probing. Analytical Chemistry, 2014, 86, 3548-3554.	6.5	101
9	Ratiometric Visualization of NO/H <sub>2</sub> S Cross-Talk in Living Cells and Tissues Using a Nitroxyl-Responsive Two-Photon Fluorescence Probe. Analytical Chemistry, 2017, 89, 4587-4594.	6.5	92
10	A novel SERS nanoprobe for the ratiometric imaging of hydrogen peroxide in living cells. Chemical Communications, 2016, 52, 8553-8556.	4.1	85
11	Target MicroRNA-Responsive DNA Hydrogel-Based Surface-Enhanced Raman Scattering Sensor Arrays for MicroRNA-Marked Cancer Screening. Analytical Chemistry, 2020, 92, 2649-2655.	6.5	78
12	Target-Activated Modulation of Dual-Color and Two-Photon Fluorescence of Graphene Quantum Dots for in Vivo Imaging of Hydrogen Peroxide. Analytical Chemistry, 2016, 88, 4833-4840.	6.5	77
13	Combination of DNA Ligase Reaction and Gold Nanoparticle-Quenched Fluorescent Oligonucleotides: A Simple and Efficient Approach for Fluorescent Assaying of Single-Nucleotide Polymorphisms. Analytical Chemistry, 2010, 82, 7684-7690.	6.5	67
14	Alkyne–DNA-Functionalized Alloyed Au/Ag Nanospheres for Ratiometric Surface-Enhanced Raman Scattering Imaging Assay of Endonuclease Activity in Live Cells. Analytical Chemistry, 2018, 90, 3898-3905.	6.5	65
15	Simultaneous Intracellular β- <scp>d</scp> -Glucosidase and Phosphodiesterase I Activities Measurements Based on A Triple-Signaling Fluorescent Probe. Analytical Chemistry, 2011, 83, 1268-1274.	6.5	64
16	Direct Fluorescent Detection of Blood Potassium by Ion-Selective Formation of Intermolecular G-Quadruplex and Ligand Binding. Analytical Chemistry, 2016, 88, 9285-9292.	6.5	63
17	Azoreductase-Responsive Nanoprobe for Hypoxia-Induced Mitophagy Imaging. Analytical Chemistry, 2019, 91, 1360-1367.	6.5	59
18	Catalytic Hairpin Self-Assembly-Based SERS Sensor Array for the Simultaneous Measurement of Multiple Cancer-Associated miRNAs. ACS Sensors, 2020, 5, 4009-4016.	7.8	57

#	Article	IF	CITATIONS
19	Design of a Room-Temperature Phosphorescence-Based Molecular Beacon for Highly Sensitive Detection of Nucleic Acids in Biological Fluids. Analytical Chemistry, 2011, 83, 1356-1362.	6.5	51
20	Fabrication of Versatile Cyclodextrin-Functionalized Upconversion Luminescence Nanoplatform for Biomedical Imaging. Analytical Chemistry, 2014, 86, 6508-6515.	6.5	51
21	Oligonucleotide Cross-Linked Hydrogel for Recognition and Quantitation of MicroRNAs Based on a Portable Glucometer Readout. ACS Applied Materials & Interfaces, 2019, 11, 7792-7799.	8.0	50
22	Poly β-Cyclodextrin/TPdye Nanomicelle-based Two-Photon Nanoprobe for Caspase-3 Activation Imaging in Live Cells and Tissues. Analytical Chemistry, 2014, 86, 11440-11450.	6.5	48
23	DNA-templated in situ growth of AgNPs on SWNTs: a new approach for highly sensitive SERS assay of microRNA. Chemical Communications, 2015, 51, 6552-6555.	4.1	44
24	Targeted Intracellular Controlled Drug Delivery and Tumor Therapy through in Situ Forming Ag Nanogates on Mesoporous Silica Nanocontainers. ACS Applied Materials & Interfaces, 2015, 7, 11930-11938.	8.0	44
25	Molecular Engineering of α-Substituted Acrylate Ester Template for Efficient Fluorescence Probe of Hydrogen Polysulfides. Analytical Chemistry, 2018, 90, 881-887.	6.5	43
26	Nanoconjugates of Ag/Au/Carbon Nanotube for Alkyne-Meditated Ratiometric SERS Imaging of Hypoxia in Hepatic Ischemia. Analytical Chemistry, 2019, 91, 4529-4536.	6.5	42
27	Azoreductase and Target Simultaneously Activated Fluorescent Monitoring for Cytochrome c Release under Hypoxia. Analytical Chemistry, 2018, 90, 5865-5872.	6.5	37
28	Poly β-cyclodextrin inclusion-induced formation of two-photon fluorescent nanomicelles for biomedical imaging. Chemical Communications, 2014, 50, 8398-8401.	4.1	35
29	Two-Photon Excitation/Red Emission, Ratiometric Fluorescent Nanoprobe for Intracellular pH Imaging. Analytical Chemistry, 2020, 92, 583-587.	6.5	34
30	Quantitative Monitoring of Hypoxia-Induced Intracellular Acidification in Lung Tumor Cells and Tissues Using Activatable Surface-Enhanced Raman Scattering Nanoprobes. Analytical Chemistry, 2016, 88, 11852-11859.	6.5	29
31	Aptamer degradation inhibition combined with DNAzyme cascade-based signal amplification for colorimetric detection of proteins. Chemical Communications, 2013, 49, 6137.	4.1	28
32	An intramolecular charge transfer (ICT)-based dual emission fluorescent probe for the ratiometric detection of gold ions. Analytical Methods, 2013, 5, 3639.	2.7	28
33	A novel AgNP/DNA/TPdye conjugate-based two-photon nanoprobe for GSH imaging in cell apoptosis of cancer tissue. Chemical Communications, 2015, 51, 16810-16812.	4.1	28
34	Hypoxia-triggered gene therapy: a new drug delivery system to utilize photodynamic-induced hypoxia for synergistic cancer therapy. Journal of Materials Chemistry B, 2018, 6, 6424-6430.	5.8	27
35	A CaO <sub>2</sub> @Tannic Acidâ€Fe <sup>III</sup> Nanoconjugate for Enhanced Chemodynamic Tumor Therapy. ChemMedChem, 2021, 16, 2278-2286.	3.2	27
36	A Sequenceâ€Selective Electrochemical DNA Biosensor Based on HRP‣abeled Probe for Colorectal Cancer DNA Detection. Analytical Letters, 2008, 41, 24-35.	1.8	26

#	Article	IF	CITATIONS
37	rGO/AuNPs/tetraphenylporphyrin nanoconjugate-based electrochemical sensor for highly sensitive detection of cadmium ions. Analytical Methods, 2018, 10, 3631-3636.	2.7	26
38	Highly selective imaging of lysosomal azoreductase under hypoxia using pH-regulated and target-activated fluorescent nanoprobes. Chemical Communications, 2019, 55, 3235-3238.	4.1	26
39	Programmable DNA triple-helix molecular switch in biosensing applications: from in homogenous solutions to in living cells. Chemical Communications, 2017, 53, 2507-2510.	4.1	25
40	Alkyne-based surface-enhanced Raman scattering nanoprobe for ratiometric imaging analysis of caspase 3 in live cells and tissues. Analytica Chimica Acta, 2018, 1043, 115-122.	5.4	25
41	Development of spiropyran-based electrochemical sensor via simultaneous photochemical and target-activatable electron transfer. Biosensors and Bioelectronics, 2014, 62, 151-157.	10.1	23
42	Alkyne/Ruthenium(II) Complex-Based Ratiometric Surface-Enhanced Raman Scattering Nanoprobe for In Vitro and Ex Vivo Tracking of Carbon Monoxide. Analytical Chemistry, 2020, 92, 924-931.	6.5	23
43	Photoactivatable Red Chemiluminescent AlEgen Probe for <i>In Vitro</i> / <i>Vivo</i> Imaging Assay of Hydrazine. Analytical Chemistry, 2021, 93, 10601-10610.	6.5	23
44	Remote-Controlled Release of DNA in Living Cells via Simultaneous Light and Host–Guest Mediations. Analytical Chemistry, 2014, 86, 10208-10214.	6.5	22
45	Upconversion Nanoprobes for in Vitro and ex Vivo Measurement of Carbon Monoxide. ACS Applied Materials & Interfaces, 2019, 11, 26684-26689.	8.0	22
46	Cyclodextrin supramolecular inclusion-enhanced pyrene excimer switching for time-resolved fluorescence detection of biothiols in serum. Biosensors and Bioelectronics, 2015, 68, 253-258.	10.1	21
47	Polycarbonate-based core-crosslinked redox-responsive nanoparticles for targeted delivery of anticancer drug. Journal of Materials Chemistry B, 2018, 6, 3348-3357.	5.8	20
48	Noninvasive and Highly Selective Monitoring of Intracellular Glucose via a Two-Step Recognition-Based Nanokit. Analytical Chemistry, 2017, 89, 8319-8327.	6.5	18
49	Synergistically enhanced multienzyme catalytic nanoconjugates for efficient cancer therapy. Journal of Materials Chemistry B, 2021, 9, 5877-5886.	5.8	18
50	Microemulsion-Confined Biomineralization of PEGylated Ultrasmall Fe <sub>3</sub> O <sub>4</sub> Nanocrystals for T2-T1 Switchable MRI of Tumors. Analytical Chemistry, 2021, 93, 14223-14230.	6.5	18
51	Hybridization-activated spherical DNAzyme for cascading two-photon fluorescence emission: Applied for intracellular miRNA measurement by two-photon microscopy. Sensors and Actuators B: Chemical, 2019, 286, 250-257.	7.8	17
52	Porous SiO2-coated Au-Ag alloy nanoparticles for the alkyne-mediated ratiometric Raman imaging analysis of hydrogen peroxide in live cells. Analytica Chimica Acta, 2019, 1057, 1-10.	5.4	17
53	A novel surface-enhanced Raman scattering-based ratiometric approach for detection of hyaluronidase in urine. Talanta, 2020, 215, 120915.	5.5	17
54	Membraneless reproducible MoS2 field-effect transistor biosensor for high sensitive and selective detection of FGF21. Science China Materials, 2019, 62, 1479-1487.	6.3	16

#	Article	IF	CITATIONS
55	Simultaneous identification of point mutations via DNA ligase-mediated gold nanoparticle assembly. Analyst, The, 2008, 133, 939.	3.5	14
56	DNA template-synthesized silver nanoparticles: A new platform for high-performance fluorescent biosensing of biothiols. Science China Chemistry, 2011, 54, 1266-1272.	8.2	14
57	Visual Biopsy by Hydrogen Peroxide-Induced Signal Amplification. Analytical Chemistry, 2016, 88, 10728-10735.	6.5	14
58	A gold nanocarrier and DNA–metal ligation-based sensing ensemble for fluorescent assay of thiol-containing amino acids and peptides. Chemical Communications, 2013, 49, 7932.	4.1	13
59	Au-Ag alloy/porous-SiO2 core/shell nanoparticle-based surface-enhanced Raman scattering nanoprobe for ratiometric imaging analysis of nitric oxide in living cells. Talanta, 2019, 205, 120116.	5.5	13
60	Cyclodextrin supramolecular inclusion-enhanced pyrene excimer switching for highly selective detection of RNase H. Analytica Chimica Acta, 2019, 1088, 137-143.	5.4	13
61	PEGylated AIEgen molecular probe for hypoxia-mediated tumor imaging and photodynamic therapy. Chemical Communications, 2021, 57, 4710-4713.	4.1	13
62	A spherical nucleic acid-based two-photon nanoprobe for RNase H activity assay in living cells and tissues. Nanoscale, 2019, 11, 8133-8137.	5.6	12
63	Biomineralization of Aggregation-Induced Emission-Active Photosensitizers for pH-Mediated Tumor Imaging and Photodynamic Therapy. ACS Applied Bio Materials, 2021, 4, 5566-5574.	4.6	12
64	Microemulsion-Confined Assembly of Magnetic Nanoclusters for pH/H <sub>2</sub> O <sub>2</sub> Dual-Responsive T <sub>2</sub> –T <sub>1</sub> Switchable MRI. ACS Applied Materials & Interfaces, 2022, 14, 2629-2637.	8.0	12
65	A plasma-polymerized film for capacitance immunosensing. Biosensors and Bioelectronics, 2004, 20, 841-847.	10.1	9
66	Peptide-fluorophore/AuNP conjugate-based two-photon excited fluorescent nanosensor for caspase-3 activity imaging assay in living cells and tissue. MedChemComm, 2017, 8, 1435-1439.	3.4	9
67	Single Molecule-Level Detection via Liposome-Based Signal Amplification Mass Spectrometry Counting Assay. Analytical Chemistry, 2022, 94, 6120-6129.	6.5	8
68	Microsphere-based suspension array for simultaneous recognition and quantification of multiple cancer-associated miRNA via DNAzyme-Mediated signal amplification. Analytica Chimica Acta, 2020, 1140, 69-77.	5.4	7
69	Self-Illuminated, Oxygen-Supplemented Photodynamic Therapy via a Multienzyme-Mimicking Nanoconjugate. ACS Applied Bio Materials, 2021, 4, 3490-3498.	4.6	7
70	Dithiocarbamate modification of activated carbon for the efficient removal of Pb( <scp>ii</scp> ), Cd( <scp>ii</scp> ), and Cu( <scp>ii</scp> ) from wastewater. New Journal of Chemistry, 2022, 46, 5234-5245.	2.8	7
71	Two-photon AgNP/DNA-TP dye nanosensing conjugate for biothiol probing in live cells. Analyst, The, 2014, 139, 6185-6191.	3.5	6
72	Two-photon excitation nanoprobe for DNases activity imaging assay in hepatic ischemia reperfusion injury. Sensors and Actuators B: Chemical, 2019, 298, 126853.	7.8	6

#	Article	IF	CITATIONS
73	Colorimetric detection of ATP with DNAzyme: design an activatable hairpin probe for reducing background signals and improving selectivity. Analytical Methods, 2014, 6, 3219-3222.	2.7	5
74	A novel DNAzyme-based paper sensor for the simple visual detection of RNase H activity. Sensors and Actuators B: Chemical, 2021, 331, 129400.	7.8	3
75	Design of multiplex logic gates: Combining regulation of DNA structure with logical calculation. Science China Chemistry, 2014, 57, 453-458.	8.2	2
76	A novel pyrene-switching aptasensor for the detection of bisphenol A. Analytical Methods, 2018, 10, 4750-4755.	2.7	2
77	A Novel DNAzyme Signal Amplification-based Colorimetric Method for RNase H Assays. Analytical Sciences, 2021, 37, 1675-1680.	1.6	2